Daylight Bactericidal Titania Textiles: A Contribution to Nosocomial Infections Control

Joana C. Matos [1,2], Cláudia Oliveira [3] and M. Clara Gonçalves [1,2,*]

[1]   Departamento de Engenharia Química, Instituto Superior Técnico, Universidade de Lisboa, 1049-001 Lisboa, Portugal; joanacmatos@gmail.com

[2]   CQE, Centro de Química Estrutural, Instituto Superior Técnico, Universidade de Lisboa, 1049-001 Lisboa, Portugal

[3]   Departamento de Biologia, CESAM, Universidade de Aveiro, Campus Universitário de Santiago, 3810-193 Aveiro, Portugal; csoliveira@ua.pt

*   Correspondence: clara.goncalves@ist.utl.pt; Tel.: +351-218419934

check for
updates

Abstract: Daylight bactericidal cotton (100% cotton) textiles are presented and proposed for future hospital use. Amorphous titania (a-TiO_2) and amorphous titania/chitosan complexes (a-TiO_2//CS) were the selected bactericidal agents. Nanoparticles (NPs) and films were the two paths designed. Cotton textiles were impregnated with a-TiO_2-based NPs or coated with a-TiO_2 films. Industrial impregnation/coating will be implemented during the textile finishing treatments. A novel (room temperature and base-catalyzed), green (hydrothermal water as a catalyst), time-saving, and easy scale-up sol–gel process was established to produce the a-TiO_2-based NPs. Amorphous-TiO_2 films were produced by a dip-in (acid catalyzed) sol–gel solution. The daylight bactericidal performance (without the need of an external ultraviolet light source) of a-TiO_2 NPs, films, and impregnated/coated textiles was proven according to AATCC 100 and ASTM E2149, using *Staphylococcus aureus* (ATCC®6538™) as the bacterial indicator strain. A bacterial reduction of 99.97% was achieved for the a-TiO_2 films and of 99.97% for the a-TiO_2//CS NPs. Regarding the impregnated textiles, a bacterial reduction of 91.66% was achieved with a-TiO_2//CS NPs, and 99.97% for cotton textiles coated with an a-TiO_2 film.

Keywords: nanoparticles; amorphous titania; chitosan; bactericidal; ASTM E2149; AATCC 100; *Staphylococcus aureus*

1. Introduction

Nosocomial infections, otherwise known as healthcare-associated infections (HCAIs), occur worldwide both in developed and developing countries, affecting approximately 8.7% of all hospitalized patients (7% in developed and 10% in developing countries), which causes prolonged hospital stay, disability, and unacceptable costs to healthcare economies [1]. According to the European Centre for Disease Prevention and Control (ECDC), three million cases of nosocomial infections occur annually, 50,000 of which are fatal [2]; thus, its control is a worldwide health priority [1–3]. Still, the growth of bacterial resistance is rendering antimicrobial agents less effective, while nosocomial pathogens (bacteria, viruses, and fungi) contaminate the surfaces and equipment handled by hospital staff, with hospital textiles being an important source of cross infections. One way to stop this dissemination is to give to textiles bactericidal properties. Thus, in order to impart them with bactericidal activity, different approaches have been purposed [4], as follows: (i) the inclusion of antimicrobial compounds in the polymeric fibers, (ii) grafting of certain moieties onto the polymer surface, or (iii) physical modification of the textile during finishing processes—the route adopted in the present work.

Oxide semiconductors, acting as photocatalysts, play a catalytic role in a wide range of cell enzymes, either generating or catalyzing reactive oxygen species (ROS), which can induce oxidative stress, damaging

cellular proteins, lipids, and DNA [5]. Crystalline TiO_2 nanoparticles (NPs) (approved by the American Food and Drug Administration for use in human food, drugs, cosmetics, and food contact materials, [6]) excel because of their photo-reactivity, photostability, reusability, inexpensively, non-toxicity, and effective bactericidal performance, which are promising for eliminating microorganisms in self-cleaning and self-sterilizing materials [7–9]. When crystalline TiO_2 is exposed to ultraviolet light ($\lambda < 400$ nm), photo-excited holes (h_{vb}^+) and electron (e_{cb}^-) charge carriers are generated. Within nanoseconds, $\approx 90\%$ of $e_{cb}^- - h_{vb}^+$ pairs recombine without any chemical effect (simply by dissipating the absorbed hv energy as heat), while $\approx 8\%$ migrate to the defects in the crystalline network (a second decay mechanism [5,6]). Only the remaining 1%–2% fraction of photo-generated charges can promote chemical reactions with surface adsorbed molecules, either generating or catalyzing ROS [5,6] (Figure 1a), which start by damaging the bacterial cells' surfaces weak points, and gradually increase cell permeability. This permeability allows for the free efflux of intracellular contents, causing cell death [10–19].
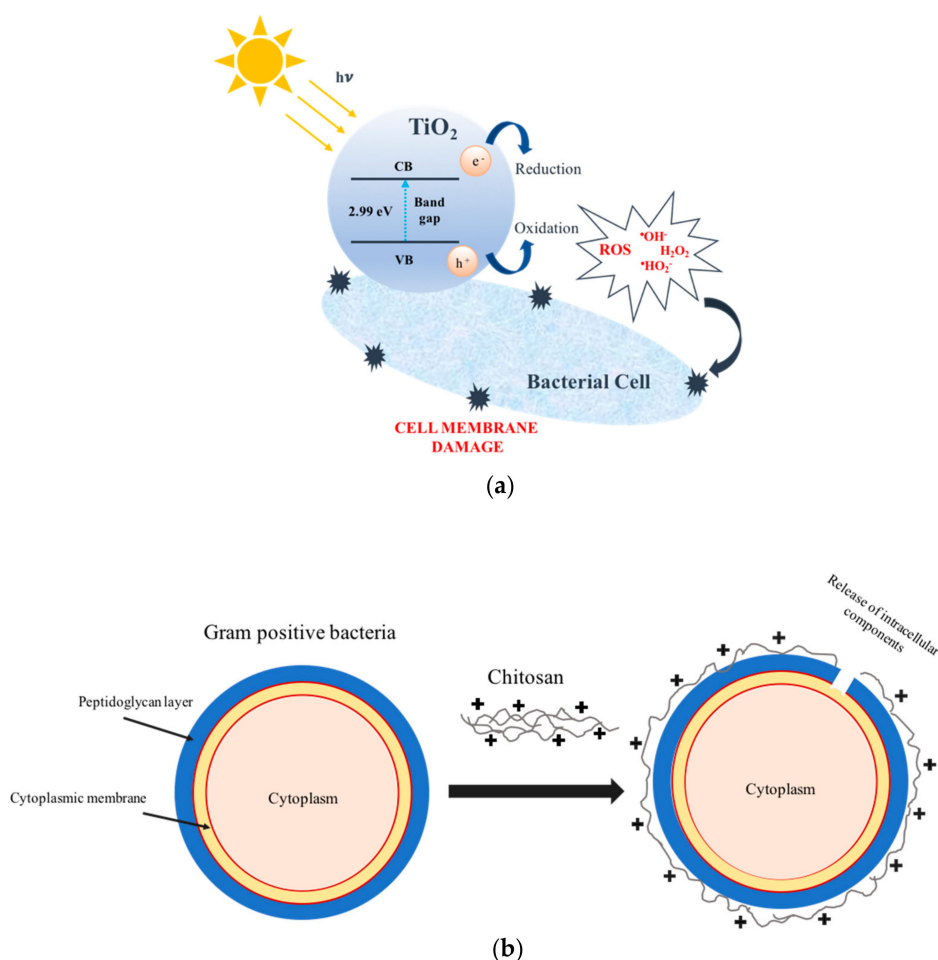

(a)

(b)

Figure 1. Damage to bacterial cell membranes induced by the following: (**a**) reactive oxygen species (ROS) generated when crystalline titania (TiO_2) is imposed to daylight and (**b**) chitosan polymer. Note: VB-valence band, CB-conduction band.

Chitosan (CS) also presents bactericidal properties. This is a versatile hydrophilic polysaccharide of animal origin found abundantly in nature and characterized by a fibrous structure. The bactericidal mechanism of CS is based on cationically-charged amino groups ($-NH^{3+}$) of glucosamine that may combine with anionic components on the Gram-positive bacteria cell surface, and may inhibit enzymes, resulting in extensive cell surface attraction, a leakage of intracellular substances, and the suppression of bacteria growth ending by damaging vital bacterial cell activities [20] (Figure 1b). Chitosan's biocompatibility, non-toxicity, non-carcinogenicity, and antimicrobial activity allows for its

use in commercial applications, such as food preservation, dentistry, and ophthalmology, and in the manufacture of wound-dressings and antimicrobial-finished textiles, namely, in cotton, polyester, and wood fibers, where patented products have reached the market (Crabyon® OMIKENSHI, Japan) [21–27]. CS amine groups present a high affinity to titania, being commonly used as a stabilizing agent for titania NPs in (water) dispersions [28]. The ultraviolet activated chitosan-(crystalline) titania bactericidal synergy has been reported in applications such as catalyst [29], protective films [30], filtration membranes [31], and biomaterials, to use as implants or in tissue engineering products [32].

This work presents a-TiO_2-based NPs (pristine a-TiO_2, a-TiO_2-NH_2, and a-TiO_2//CS) synthesized by a novel, room-temperature, base-catalyzed, green (ammonia-free) sol–gel protocol. TiO_2 films were also used, which were synthesized by a classical acid catalyzed sol–gel process [33]. NP and film morphology, a lack of crystallinity, and structural characterization were performed through transmission electron microscopy (TEM), X-ray analysis (XRD), and Fourier transform infrared spectroscopy (FTIR). The daylight bactericidal properties (without the need for an external ultra-violet light source) of the obtained NPs/films were evaluated according the ASTM E2149 test method. The second part of this work illustrates the application of a-TiO_2 products to the textile industry, where a cost-effective, easy scale-up process was developed, and a daylight bactericidal commodity was achieved. The daylight bactericidal performance (without the need of external ultra-violet light source) of impregnated or coated textiles with titania NPs/films, was evaluated according to the AATCC 100 test method, using *Staphylococcus aureus* (*S. aureus*, ATCC®6538[TM]) as reference test strain.

2. Materials and Methods

2.1. Materials

All chemicals—aqueous sodium silicate solution (SSS; $Na_2O.SiO_2$, 27% wt. % SiO_2), titanium IV isopropoxide (TiPOT, 97%), 3-aminopropyltriethoxysilane (APTES; 99%), tetraethyl orthosilicate (TEOS; ≥99%), chitosan (50,000 to 190,000 Da, 75%–85% deacetylate), and nitric acid ($HNO_3 \geq 65\%$)—were purchased from Sigma-Aldrich (Darmstadt, Germany), and were used without further purification. Absolute ethanol (EtOH; 99.5%), from Merck (Darmstadt, Germany); bi-distilled water (conductivity 0–2 µS/cm^3, pH 5.8–6.5); and hydrothermal water (SPA, Cabeço de Vide, Portugal) were also used. Acetic acid glacial (CH_3COOH; 99+%) was purchased from Alfa Aesar (Ward Hill, USA), and hydrochloric acid was purchased (HCl, 35%–38%) from Sigma-Aldrich (Darmstadt, Germany),

Cotton (100% cotton) fabric, 120 g/m^2 basis weight, was supplied by CITEVE, Portugal. Microbiology culture media, Luria broth (LB), and Luria agar (LA) were purchased from VWR (USA).

2.2. Experimental Methodology

The daylight bactericidal performance (without the need of external ultra-violet light source) of a-TiO_2 (impregnated/coated) cotton (100% natural fibers) textiles was studied. Two main routes (A and B) were evaluated (Figure 2), namely:

Route A (Figure 2, Route A)

a.   Novel synthesis of a-TiO_2 NPs (room temperature, sol-gel, base-catalyzed, eco-friendly protocol):

       a.1   pristine a-TiO_2 NPs (A.1.)
       a.2   in situ amine-functionalized amorphous titania (a-TiO_2-NH_2) NPs (A.1.)
       a.3   ex situ CS-decorated amorphous titania (a-TiO_2//CS) NPs (A.1.)

b.   Textile impregnation with a-TiO_2 based NPs, to be industrially implemented as a finishing process (A.3.)

c.   Daylight bactericidal performance of NPs and impregnated cotton textiles according to ASTM E 2149 and AATCC 100 test methods using S. aureus (ATCC®6538TM) as bacterial indicator strain (A.2., A.4.)

Route B (Figure 2, Route B)

d.   TiO$_2$ (acid-catalyzed) sol-gel solution preparation (B.1.)
e.   Textile coating with a-TiO$_2$ film by dip in sol-gel solution, to be industrially implemented as a finishing process (B.3.)
f.   Daylight bactericidal performance of films and coated cotton textiles according to ASTM E 2149 and AATCC 100 test methods using S. aureus (ATCC$^®$6538TM) as bacterial indicator strain (B.2., B.4.).

Steps b and e were performed with and without cure, so to test the role of temperature on the NPs'/films' adhesion to the textile, according to the authors' previous work [34]. The NPs were characterized by TEM, FTIR, and XRD, and were impregnated/coated textiles by SEM and FTIR.
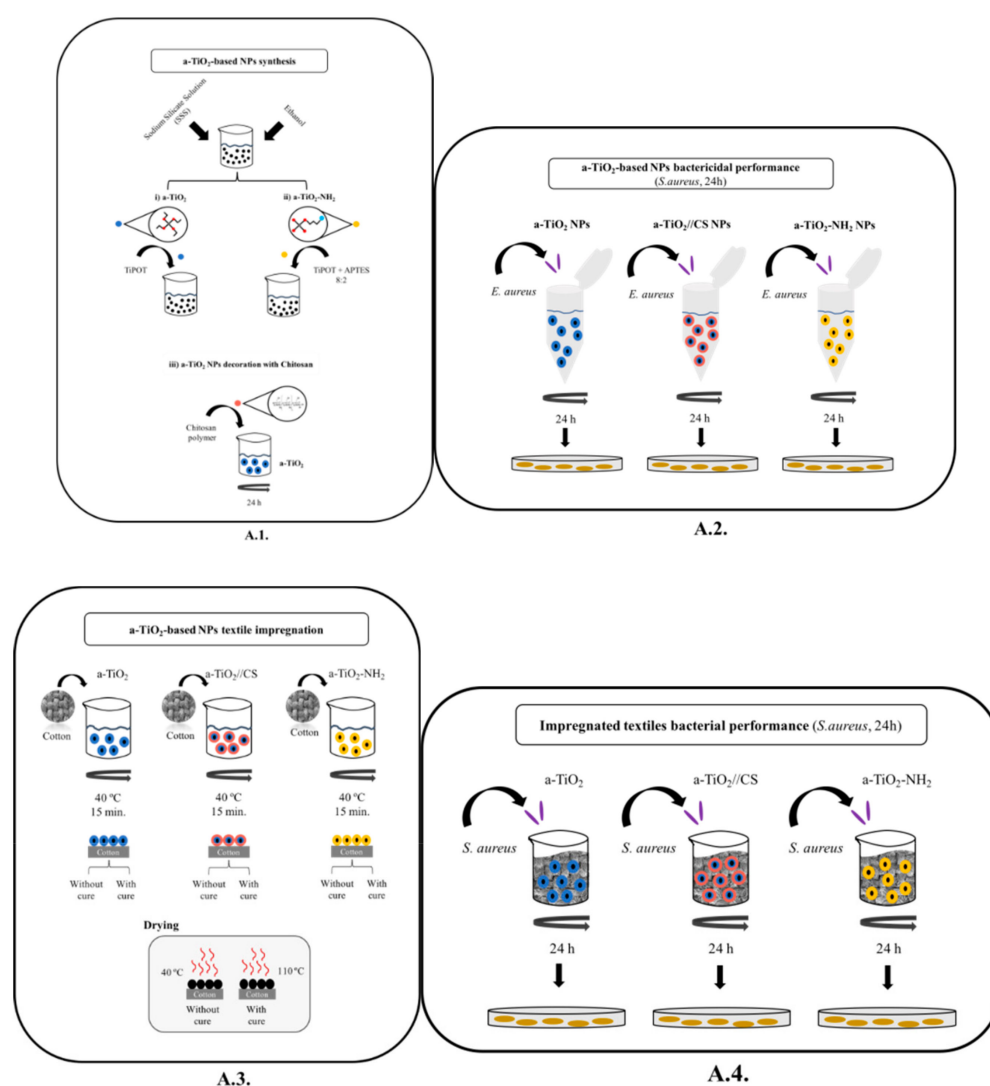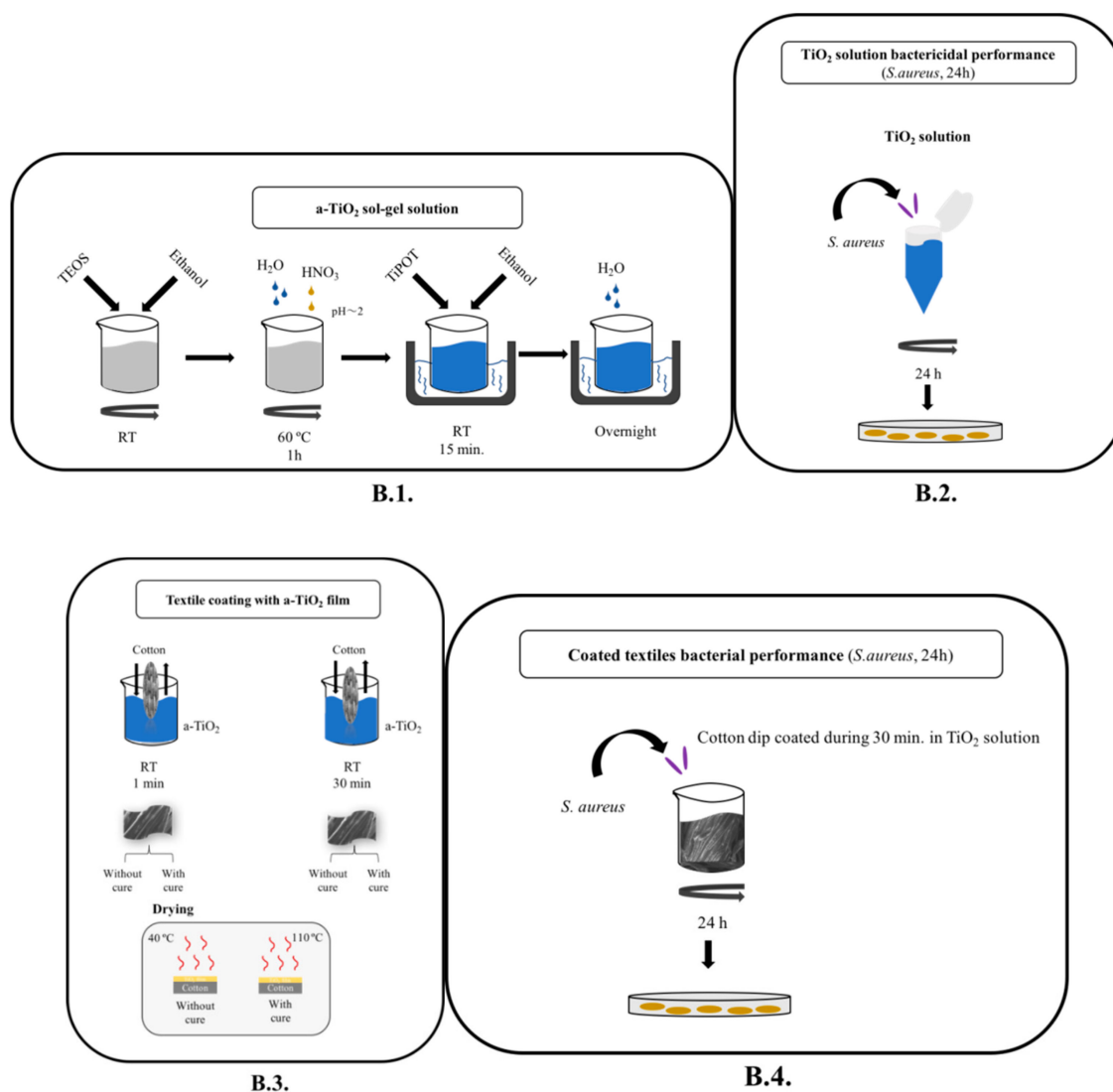
Route A

Figure 2. *Cont.*

Route B

Figure 2. Process flowchart, namely: Route A (sol-gel NPs synthesis and textiles impregnation with NPs) and Route B (sol-gel film synthesis and textiles coating). Note: RT-room temperature; C-chitosan; TEOS-tetraethyl orthosilicate

2.2.1. Amorphous Titania Nanoparticles Synthesis

In this work, pristine a-TiO$_2$ NPs were synthesized for the first time through a room temperature, alkaline (base-catalyzed), and eco-friendly (ammonia free) sol-gel protocol, where hydrothermal water (SPA Cabeço de Vide, Cabeço de Vide, Portugal, pH ≈11) was used as a catalyst [34]. Briefly, a volume of 280 μL of sodium silicate solution (SSS; as nucleating agent) was diluted in 25 mL of absolute ethanol, and the resulting solution was placed under magnetic stirring for 15 min. A mixture of ethanol and hydrothermal water was then added to the suspension, and was stirred for 15 min. After this time, the suspension was placed in the ultrasound and 500 μL of titanium isopropoxide (TiPOT) was added, followed by 30 min of sonication.

In situ amine functionalization (a-TiO$_2$-NH$_2$ NPs) was performed according to the methodology described above. After titanium isopropoxide sonication (for 30 min), a volume of APTES was added and the mixture was left in magnetic stirring for 24 hours at room temperature. A molar ratio of 8:2 TiPOT to APTES was used.

Chitosan decoration was performed ex situ (a-TiO$_2$//CS NPs). The chitosan was solubilized in glacial acetic acid at 50 mM, based on the literature [24]. The NPs suspension was prepared by suspending 8 mg of a-TiO$_2$ NPs (suspension 1) in 5 mL of absolute ethanol. Finally, 20 mL of CS (corresponding to 20 mg of CS) was added to the suspension. The mixture was left in magnetic stirring for 24 h at room temperature. The NPs and films acronyms and compositions are presented in Table 1.

Table 1. Amorphous titania (a-TiO$_2$)-based nanoparticles (NPs) and films acronyms, compositions, and sol-gel precursor's volumes. CS-chitosan; APTES-3-aminopropyltriethoxysilane; TiPOT-titanium IV isopropoxide.

Acronym	Precursors	V_{TiPOT}:V_{Prec}(µL)	Catalyst
a-TiO$_2$ NPs	TiPOT	500	Hydrothermal water pH ≈ 11
a-TiO$_2$-NH$_2$ NPs	TiPOT:APTES 8:2	TiPOT: 417 APTES: 83	Hydrothermal water pH ≈ 11
a-TiO$_2$ film	TiPOT	830	Nitric acid pH ≈ 2
Acronym	Decoration	NPs:Decoration amount	
a-TiO$_2$/CS NPs	Chitosan	10 mg NPs + 25 mg CS	

2.2.2. TiO$_2$ Solution Preparation

A settled (acid-catalysed) sol–gel protocol was used for the preparation of the TiO$_2$ sol–gel solution [33]. Briefly, 2.5 mL of TEOS was mixed with 1.5 mL of ethanol under magnetic stirring. Then, 0.25 mL of H$_2$O (drop by drop) and two drops of HNO$_3$ (or until pH ≈ 2) were added. The mixture was left in magnetic stirring for 1 h at 60 °C. After this time, 5 mL of ethanol and 0.83 mL of TiPOT were added. The mixture was placed under ultrasound for 15 min. Finally, 0.55 mL of bidistilled H$_2$O was added to the mixture (drop by drop) and left overnight in magnetic stirring.

The a-TiO$_2$ textile film was prepared through dip-coating. The film acronyms and compositions are presented in Table 1.

2.2.3. Textile Impregnation/Coating

The textile impregnation and coating were performed following the protocol (Figure 2):

1. Textile impregnation with amorphous titania-based NPs (a-TiO$_2$, a-TiO$_2$-NH$_2$, and a-TiO$_2$//CS; Figure 2A.3).
2. The textile impregnation was performed with 0.5% (in weight) on a cotton textile (according to the Portuguese Standard ISO 105-C06, 1994, see details in the literature [34]). Shortly, 25 mg of a-TiO$_2$ NPs were suspended in 50 mL of distilled water, and were sonicated for 30 min. Then, 5 g of cotton textile (100% cotton) was immersed in the colloidal suspension, under magnetic stirring, at 40 °C for 15 min.
3. Textile coating with a titania solution (a-TiO$_2$ film; Figure 2B.3).
4. Briefly, the cotton textile was immersed in the TiO$_2$ sol–gel solution (at a constant rate of 2 cm/min) and then pulled up (also at the same rate). An a-TiO$_2$ coating forms, its thickness being determined by the withdrawal rate (being inversely proportional). During the deposition and drainage steps, the solvent (alcohol) and the excess/unreacted reagents (water and/or silica/titania precursors) evaporate.
5. The impregnation/coating was performed without cure (woven at 40 °C, for 24 h) and with cure (at 110 °C, for 1h) to enhance the NPs'/films' adhesion to the cotton textile [34].

2.3. Physical Characterization

2.3.1. Transmission Electron Microscopy (TEM)

The morphology, size (static diameter), and size distribution of the synthesized a-TiO$_2$-based NPs were assessed by transmission electron microscopy (TEM). A Hitachi H-8100 model was used, and the micrographs were obtained using an applied tension of 200 kV. This model is a conventional TEM with a high brightness LaB6 electron source and large specimen-tilt (>30°) capabilities. To prepare a TEM sample, a drop of the NPs suspension was placed on a copper grid and dried at room temperature.

2.3.2. Fourier Transform Infrared Spectroscopy (FTIR)

Amorphous-TiO$_2$-based NPs and powder films were analyzed by Fourier transform infrared spectroscopy (FTIR). FTIR was performed with potassium bromide pellets (KBr, ≥99+%, FTIR grade, from Sigma-Aldrich). Amorphous TiO$_2$-based NPs and films were finely ground and mixed with potassium bromide, and then pressed into a disc (5 mg a-TiO$_2$-based NPs or film to 200 mg KBr). The KBr pellet was used as a background. The Nicolet 5700 model was used in transmission mode, through a KBr beamsplitter.

2.3.3. X-ray Powder Diffraction (XRD)

To confirm the amorphous character of the synthesized NPs and films, powder X-ray diffraction (XRD) was used. The diffractograms were obtained with a PANalytical X'Pert Pro diffractometer using Cu-Kα radiation. The data were collected in steps of 0.02° in the 20°–80° range (2θ), with a counting time per step of 4 s.

2.3.4. Scanning Electron Microscopy (SEM)

Textile impregnation/coating efficiency was semi-quantitatively evaluated through field emission SEM. A JEOL JSM-7001F model, operated with a 15.0 kV accelerating voltage, was used. A simple random sampling (impregnated/coated cotton textile) without replacement was performed, and a minimum of 50 mm^2 was observed for each set of textile nanocomposite (without and with cure). The textile samples were coated with a ≈80 nm layer of gold/palladium prior to the SEM observation.

2.4. Daylight Bactericidal Performance Evaluation

To determine the daylight bactericidal activity (without the need for an external ultra-violet light source) of the NPs/films and impregnated/coated textiles, assays based on the guidelines of the standard test methods of ASTM E 2149 and AATCC 100 were performed. The methods use a dynamic contact assay, where the immobilized antibacterial agent (a-TiO$_2$-based NPs/films and impregnated/coated textiles) is incubated for 24 h with test strain cell suspensions (*S. aureus*, ATCC®6538^{TM} (Figure 2A.2,A.4,B.2,B.4). After incubation, the bacterial cells were plated and counted. Briefly, the procedure was carried out as follows: the bacterial cells of *S. aureus* were grown in Tryptic Soy Broth (TSB) for 24 h at 35 °C, and diluted using a KH$_2$PO$_4$ (0.3 mM) buffer solution to achieve a concentration from 1.5×10^5 UCF/mL to 3×10^3 UCF mL^{-1} (pH ≈ 7.3). The amount of NPs and film (in powder) tested in this assay was 0.061 ± 0.001 g, and 1 ± 0.1 g for the impregnated/coated textile samples (after weighting, the textile was finely cut). The samples were introduced in the Schott flaks, previously prepared, which were then placed in a wrist-shaker in daylight and at room temperature for 24 h (winter day cycle, 6 h day/18 h night). No artificial UV stimuli were induced. The bacterial reduction was calculated using a standard pour plate technique. At the beginning and end of the assay, 1 mL was drawn from each flask, doing successive dilutions of 1:10. The aliquots of each sample were seeded over culture plates with Luria agar (LA) medium in triplicates, which were then incubated for 20–24 h at 35 °C. For the determination of the bacterial reduction, the Colony Forming Units (CFU) were

counted and the percentage of reduction, R (%), was quantified by the expression given in Equation (1). C_0 represents the CFU of the control sample and C corresponds to the CFU of the analyzed material.

$$R\ (\%) = \frac{(C_0 - C)}{C_0} \times 100\% \tag{1}$$

The control assays were performed by incubating the bacterial cells in the absence of any kind of TiO_2 or chitosan material. Briefly, the bacterial cells were incubated with the following: (i) buffer solution (negative control), (ii) NPs without a bactericidal performance or textile matrix with a reference bactericidal (positive control), and finally (iii) TiO_2-based NPs/film under analysis. Triplicate assays were performed.

3. Results and Discussion

This work presents, for the first time, a room temperature, (eco-friendly) alkaline route sol–gel synthesis of TiO_2-based NPs. Pristine a-TiO_2 NPs, in situ amine-functionalized a-TiO_2-NH_2 NPs, and ex situ CS decorated a-TiO_2//CS NPs (Table 1) were the synthesized compositions. Amine groups were used as the bonding strategy between a-TiO_2 NPs and cotton textiles [34]. The chitosan (CS) polymer should provide an even higher surface bonding capacity towards single-handed a-TiO_2-NH_2 NPs, because of the presence of the amine, acetate, and hydroxyl groups. Nevertheless, CS was primarily chosen to reinforce the bactericidal performance of TiO_2, according on the synergetic effects reported in the literature [20–26].

3.1. NPs Characterization

The surface area to volume ratio is central when it comes to surface properties. The NP size, size distribution, and morphology were studied. Figure 3A–C shows the TEM images of a-TiO_2, a-TiO_2-NH_2, and a-TiO_2//CS NPs, respectively. These images show that the synthesized NPs are monosized and spherical (static diameter $\approx$3–4 nm $\pm$ 0.1 nm), with the spherical morphology being the first sign of the amorphous character of TiO_2 NPs [35].
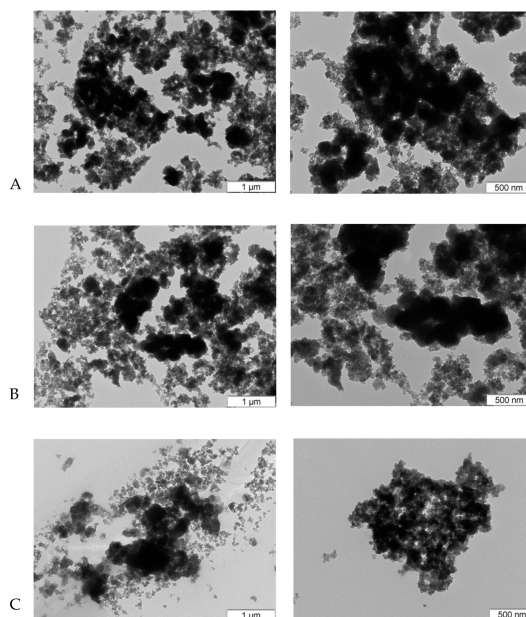

Figure 3. Transmission electron microscopy (TEM) images of a-TiO_2-based nanoparticles (NPs), namely: (**A**) a-TiO_2 NPs, (**B**) a-TiO_2-NH_2NPs, and (**C**) a-TiO_2/CS NPs. (for each composition two different amplifications are shown—1 μm and 500 nm).

FTIR prove the presence of TiO_2, amine groups and CS (Figure 4). The main FTIR TiO_2 peak, centered at 526 cm^{-1} and assigned to the vibration of Ti-O bond [36], is present in all spectra, although no peaks assigned to Ti-O-Ti (600-400 cm^{-1}, $\approx$550 cm^{-1}, $\approx$342 cm^{-1}) [36–38] were detected. In the case of a-TiO_2-NH_2 NPs spectrum a peak at 1510 cm^{-1}, assigned to C-N bonds, and a slight shoulder at $\approx$2940 cm^{-1}, assigned to C-H stretching were observed, proving the a-TiO_2 NPs amine-functionalization. A-TiO_2-NH_2 NPs (the only hybrid matrix, TiPOT:APTES 8:2) does not exhibit typical Si-O-Ti peak at $\approx$949 cm^{-1} [36]. In the FTIR spectra of a-TiO_2//CS NPs peaks in the range 1070–1020 cm^{-1} and 2900 cm^{-1} are assigned to C-O and C-H stretching, respectively, confirming the presence of CS polymer.
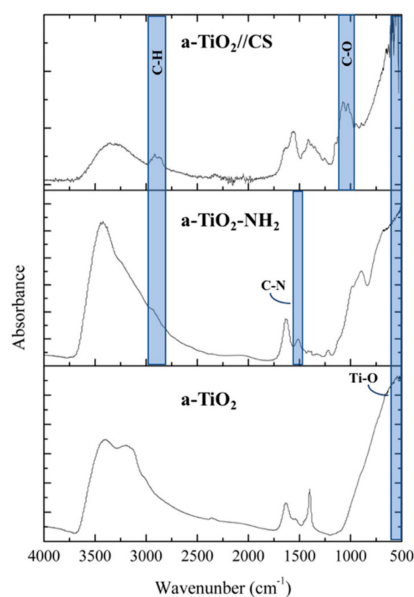

Figure 4. Fourier transform infrared spectroscopy (FTIR) spectra of a-TiO_2-based NPs.

XRD characterizations confirm the amorphous character of all of the TiO_2 NPs (a-TiO_2, a-TiO_2-NH_2, and a-TiO_2//CS) and films (Figure 5), as no defined or sharp peaks were observed in the diffractograms. Chitosan ex situ decoration of the a-TiO_2 NPs did not affect the NPs' amorphous character.
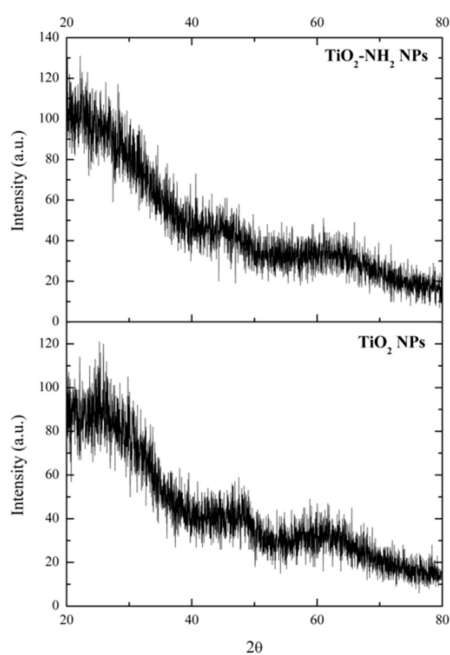

Figure 5. X-ray analysis (XRD) diffractograms of a-TiO_2 and a-TiO_2-NH_2 NPs.

3.2. NPs Textile Impregnation Efficiency

All of the studied a-TiO$_2$-based NPs bind to the cotton textile. Figure 6 shows the SEM images of the cotton textile impregnated with amorphous pristine (A and B) and amine-functionalized (C and D) titania NPs.
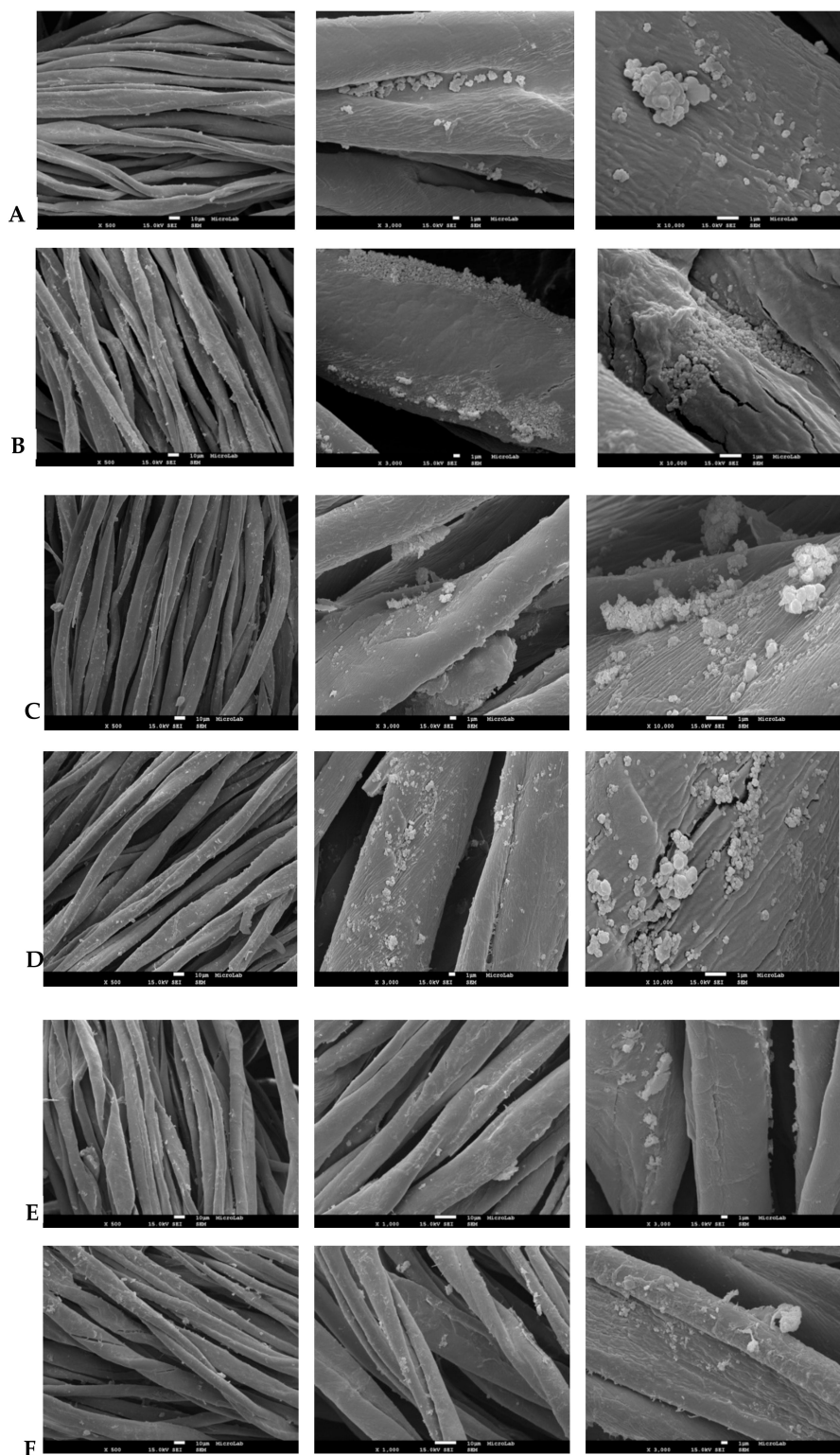

Figure 6. SEM images of cotton matrix impregnated with the following: a-TiO$_2$ NPs (**A**-without cure; **B**-cured); a-TiO$_2$-NH$_2$ NPs (**C**-without cure; **D**-cured), and a-TiO$_2$//CS NPs (**E**-without cure; **F**-cured).

Compared to pristine a-TiO$_2$ NPs, a higher impregnation efficiency of amino-functionalized NPs (a-TiO$_2$-NH$_2$ NPs) was expected, in accordance with the author's previous work [34]. The cure process is also supposed to enhance the NPs bidding efficiency [34]. Notwithstanding, in the present study, the amine-functionalization or cure did not boost the binding efficiency of the NPs to the textile.

Figure 6E,F also presents the SEM images of the cotton textiles impregnated with a-TiO$_2$//CS NPs (cure and without cure). Compared to a-TiO$_2$, a more efficient matrix coverage (higher number of NPs per unit area) was achieved. Here, the amine, acetate, and hydroxyl groups from the CS polymer do play an active role in cotton adhesion (through second order chemical bonding), offering higher bonding possibilities. Regarding the cure step, the SEM images reveal no significant difference between the cured and non-cured samples.

3.3. Film Textile Coating Efficiency

Figure 7 shows a cotton textile coated with an a-TiO$_2$ film, where a complete coverage of the textile matrix was successfully achieved. The immersion time did not play any role in cotton textile coverage (1 min and 30 min) efficiency.
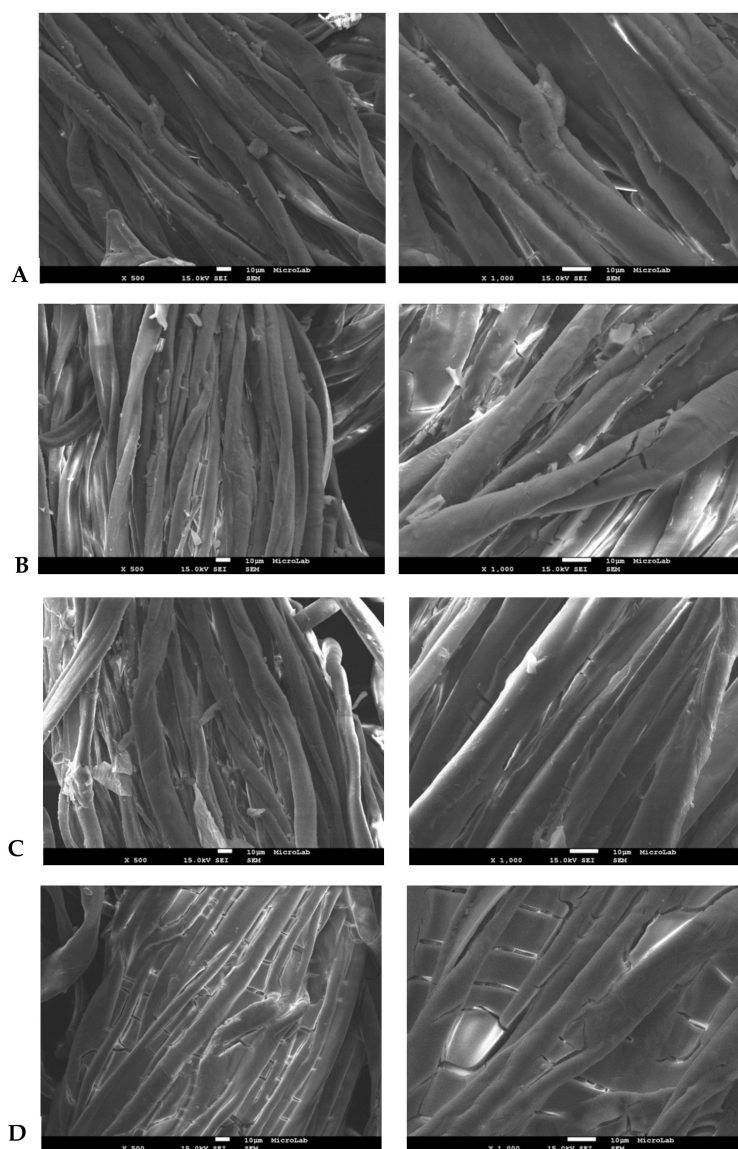

Figure 7. Cotton matrix coated with a-TiO$_2$ film, as follows: after 1 min immersion (**A**-without cure; **B**-cured) and after 30 min immersion (**C**-without cure; **D**-cured).

3.4. Daylight Bactericidal Performance of NPs/Films and Impregnated/Coated Textiles

S. aureus is a major bacterial human pathogen that may cause a large variety of clinical symptoms. *S. aureus* transmission is typically from direct contact, from infections common in community-acquired and hospital-acquired settings [39,40].

In this work, the bactericidal properties of a-TiO$_2$-based NPs were determined after 24h of incubation with the *S. aureus* cell suspension (ASTM E 2149 test method) at daylight (without any UV light exposition or stimuli), and by the determination of the cell reduction values for each of the NPs tested. Amorphous TiO$_2$ NPs exhibited an antimicrobial efficiency above 90% of bactericidal reduction (Figure 8). Amine-functionalization slightly decreases the NPs bactericidal performance to 86.89%, which is attributed to NPs agglomeration (Figure 6C,D) and amine steric effects [41], both reducing the interface area between the NPs and bacteria.
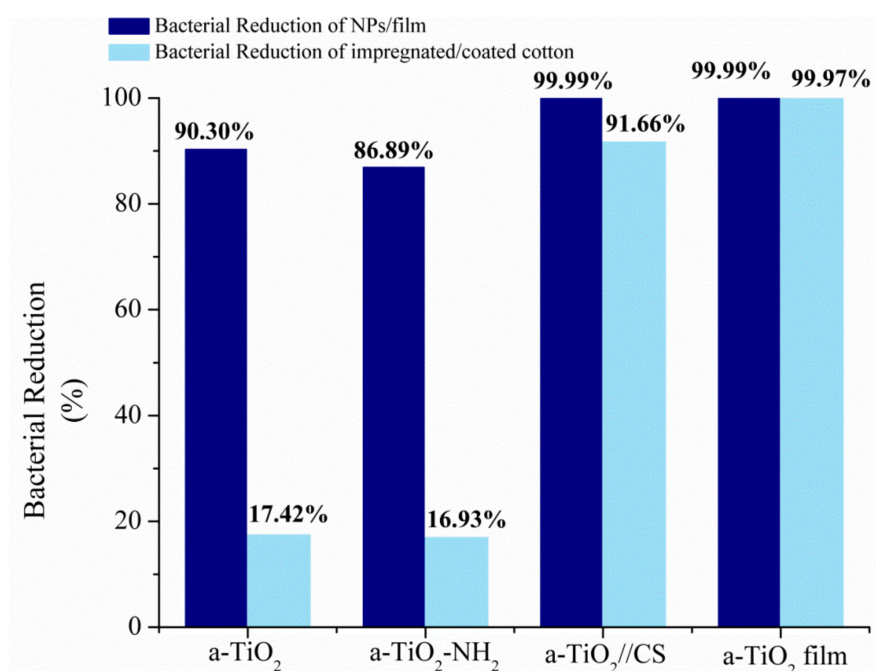

Figure 8. Daylight bacterial reduction of *S. aureus* achieved by a-TiO$_2$ NPs/films and impregnated/coated cotton textiles.

Chitosan has been conjugated with a-TiO$_2$ NPs to test the synergistic effect on the viability of *S. aureus*. CS decoration raised the bacterial performance to 99.99% (Figure 6), in accordance with the reported results in (crystalline) titania-chitosan complexes [28,42].

The a-TiO$_2$-based NPs/films showed daylight bactericidal efficiency in the following order:

a-TiO$_2$ film ≈ a-TiO$_2$//CS NPs > a-TiO$_2$ NPs > a-TiO$_2$-NH$_2$ NPs.

Regarding the textiles impregnated/coated with a-TiO$_2$ NPs/films, the bactericidal performance was also determined after 20–24 h of incubation with the bacterial cell suspension of *S. aureus* (AATCC 100 test method). The tests were performed with natural daylight (24 h, natural day cycle of 8 h day/16 h night), without the use of any artificial UV lamps or any UV stimuli (during or before to the tests).

A bactericidal reduction of 17.42% was observed in the cotton textiles impregnated with a-TiO$_2$ NPs, representing an enormous loss of bactericidal efficiency towards the equivalent NPs (90.30% bacterial reduction). When it comes to the textiles impregnated with amine-functionalized NPs, a bacterial reduction of 16.93% was observed, replicating the previous discouraging behavior. Only the assay performed with TiO$_2$//CS impregnation exhibited a successful reduction on the bacterial cell

colonies, of 91.66% (Figure 6). In the textiles impregnated with CS-TiO$_2$ NPs, any coverage inefficiency will be outstripped by the CS-TiO$_2$ synergetic bactericidal performance.

The cotton textile coated with a a-TiO$_2$ film exhibited the highest daylight bactericidal activity with a >99.97% bacterial reduction. Here, the complete textile coverage proves the high daylight bactericidal activity of the a-TiO$_2$ structures. It may be concluded that the coverage ratio plays a determinant role in the textile's bactericidal activity.

Titania cotton textiles showed a daylight bactericidal efficiency in the following order:

$$a\text{-TiO}_2 \text{ film} > a\text{-TiO}_2//\text{CS NPs} >>> a\text{-TiO}_2 \text{ NPs} \approx a\text{-TiO}_2\text{-NH}_2 \text{ NPs}.$$
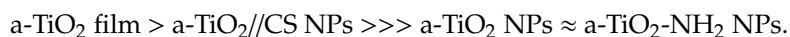
4. Conclusions

Daylight bactericidal cotton textiles were developed, aimed at hospital use. Amorphous titania NPs were synthesized through a room temperature, base catalyzed, eco-friendly, easy-scalable sol–gel process, addressing textile impregnation during industrial finishing processes. Titania film synthesis followed the classical acid catalyzed route. Successful textile impregnation with a-TiO$_2$-based NPs and textile coating with titania film drive to titania-cotton matrixes.

The daylight bactericidal performance of the NPs/films and impregnated/coated cotton textiles were validated according to the AATCC 100 and ASTM E2149 test methods, using *S. aureus* (ATCC$^{®}$6538^{TM}) as the bacterial indicator strain. The titania NPs' and films' daylight bactericidal efficiency was observed according to the following order: a-TiO$_2$ film $\approx$ a-TiO$_2$//CS NPs > a-TiO$_2$ NPs > a-TiO$_2$-NH$_2$ NPs, following the sequence for the titania textiles, namely: a-TiO$_2$ film > a-TiO$_2$//CS NPs >>> a-TiO$_2$ NPs $\approx$ a-TiO$_2$-NH$_2$ NPs.

The absence of any UV light or stimuli during the laboratorial bactericidal tests should be emphasized. Amorphous titania NPs/films and impregnated/coated textiles exhibited a bactericidal performance in natural daylight, being an industrially promising, constituting a cost-effective and technological affordable disinfection method that may be particularly useful in hospital and health services units. Furthermore, it is important to highlight that (i) amorphous oxides (NPs and films) usually present higher water and body fluids solubility, and therefore a lower toxicity, than the correspondent crystalline forms (which are commonly insoluble in water and body fluids, due to their lower Gibbs free energy values, discussed in the literature [43]), and (ii) the impregnation method simulates the domestic washing machine cycle, allowing for an easy, low-cost hospital re-charge of textiles.

References

1. Girard, R.; Perraud, M.; Prüss, A.; Savey, A.; Tikhomirov, E.; Thuriaux, M.; Vanhems, P. *Prevention of Hospital-Acquired Infections: A Practical Guide. World Health Organization*, 2nd ed.; Ducel, G., Fabry, J., Nicolle, L., Eds.; World Health Organization: Geneva, Switzerland, 2002.

2. ECDC, European Centre for Disease Prevention and Control, An agency of the European Union, Communicable Disease Threats Reports. Available online: https://ecdc.europa.eu/en/home (accessed on 24 April 2019).

3. World Health Organization (WHO). *Global Antimicrobial Resistance Surveillance System: Manual for Early Implementation*; World Health Organization: Geneva, Switzerland, 2015.

4. Morais, D.S.; Guedes, R.M.; Lopes, M.A. Antimicrobial Approaches for Textiles: From Research to Market. *Materials* **2016**, *9*, 498. [CrossRef]

5.　Arora, H.; Doty, C.; Yuan, Y.; Boyle, J.; Petras, K.; Rabatic, B.; Paunesku, T.; Woloschak, G. Nanomaterials for the Life Sciences. In *Nanocomposites*; Kumar, C.S.S.R., Ed.; WILEY-VCH Verlag GmbH & Co. KGaA: Weinheim, Germany, 2010; Volume 8, p. 1.

6.　FDA U.S. Food & Drug Administration. CFR—Code of Federal Regulations Title 21. Available online: https://www.accessdata.fda.gov/scripts/cdrh/cfdocs/cfcfr/cfrsearch.cfm (accessed on 1 April 2018).

7.　Fujishima, A.; Honda, K. Electrochemical Photolysis of Water at a Semiconductor Electrode. *Nature* **1972**, *238*, 37–38. [CrossRef]

8.　Banerjee, S.; Dionysiou, D.D.; Pillai, S.C. Self-Cleaning Applications of TiO2 by Photo-Induced Hydrophilicity and Photocatalysis. *Appl. Catal. B* **2015**, *176–177*, 396–428. [CrossRef]

9.　Gonçalves, M.C.; Pereira, J.C.; Matos, J.; Vasconcelos, H.C. Antimicrobial and Photocatalytic Application of Amorphous Titania: A Paradigma Change. *Molecules* **2018**, *23*, 1677. [CrossRef] [PubMed]

10.　Bianchi, M.G.; Allegri, M.; Chiu, M.; Costa, A.L.; Blosi, M.; Ortelli, S.; Bussolati, O.; Bergamaschi, E. Lipopolysaccharide Adsorbed to the Bio-Corona of TiO2 Nanoparticles Powerfully Activates Selected Pro-Inflammatory Transduction Pathways. *Front. Immunol.* **2017**, *8*, 866. [CrossRef] [PubMed]

11.　Bonyadi, Z.; Mirzaee, M.; Ejtehadi, M.M.; Mokhtari, M. The Bactericidal Effect of Simultaneous Titanium Oxide on Common Hospital Bacteria. *Environ. Monit. Assess.* **2017**, *189*, 342. [CrossRef]

12.　Fagan, R.; McCormack, D.E.; Dionysiou, D.D.; Pillai, S.C. A Review of Solar and Visible Light Active TiO2 Photocatalysis for Treating Bacteria, Cyanotoxins and Contaminants of Emerging Concern. *Mater. Sci. Semicond. Proc.* **2016**, *42*, 2–14. [CrossRef]

13.　Leyland, N.S.; Podporska-Carrol, J.; Browne, J.; Hinder, S.J.; Quilty, B.; Pillai, S.C. Highly Efficient F, Cu Doped TiO2 Anti-Bacterial Visible Light Active Photocatalytic Coatings to Combat Hospital-Acquired Infections. *Sci. Rep.* **2016**, *6*, 24770. [CrossRef] [PubMed]

14.　Etacheri, V.; Valentin, C.D.; Schneider, J.; Bahnemann, D.; Pillai, S.C. Visible-Light Activation of TiO2 Photocatlysts: Advances in Theory and Experiments. *J. Photochem. Photobiol. C* **2015**, *25*, 1–29. [CrossRef]

15.　Jesline, A.; John, N.P.; Narayanan, P.M.; Vani, C.; Murugan, S. Antimicrobial Activity of Zinc and Titanium Dioxide Nanoparticles Against Biofilm-Producing Methicillin-Resistant Staphylococcus Aureus. *Appl. Nanosci.* **2015**, *5*, 157–162. [CrossRef]

16.　Pelaez, M.; Nolan, N.T.; Pillai, S.C.; Seery, M.K.; Falaras, P.; Kontos, A.G.; Dunlop, P.S.M.; Hamilton, J.W.J.; Byrne, J.A.; O'Shea, K.; et al. A Review on the Visible Light Active Titanium Dioxide Photocatalysts for Environmental Applications. *Appl. Catal. B Environ.* **2012**, *125*, 331–349. [CrossRef]

17.　Liou, J.-W.; Chang, H.-H. Bactericidal Effects and Mechanisms of Visible Light-Responsive Titanium Dioxide Photocatalysts on Pathogenic Bacteria. *Arch. Immunol. Ther. Exp.* **2012**, *60*, 267–275. [CrossRef] [PubMed]

18.　Visai, L.; De Nardo, L.; Punta, C.; Melone, L.; Cigada, A.; Imbriani, M.; Arciola, C.R. Titanium Oxide Antibacterial Surfaces in Biomedical Devices. *Int. J. Artif. Organs* **2011**, *34*, 929–946. [CrossRef]

19.　Huang, Z.; Blake, D.M.; Maness, P.-C.; Wolfrum, E. Bactericidal Mode of Titanium Dioxide Photocatalysis. *J. Photochem. Photobiol. A Chem.* **2000**, *130*, 163–170. [CrossRef]

20.　Raafat, D.; Bargen, K.; Haas, A.; Sahl, H.-G. Insights into the Mode of Action of Chitosan as an Antibacterial Compound. *Appl. Environ. Microbiol.* **2008**, *74*, 3764–3773. [CrossRef] [PubMed]

21.　Nilsen-Nygaard, J.; Strand, S.P.; Vårum, K.M.; Draget, K.I.; Nordgård, C.T. Chitosan: Gels and Interfacial Properties. *Polymers* **2015**, *7*, 552–579. [CrossRef]

22.　Raafat, D.; Sahl, H.-G. Chitosan and Its Antimicrobial Potential—A Critical Literature Survey. *Microb. Biotechnol.* **2009**, *2*, 186–201. [CrossRef] [PubMed]

23.　Kong, M.; Chen, X.G.; Xing, K.; Park, H.J. Antimicrobial Properties of Chitosan and Mode of Action: A State of the Art Review. *Int. J. Food Microbiol.* **2010**, *144*, 51–63. [CrossRef]

24.　Deng, Z.; Zhen, Z.; Hu, X.; Wu, S.; Xu, Z.; Chu, P. Hollow Chitosan-Silica Nanospheres as pH-Sensitive Targeted Delivery Carriers in Breast Cancer Therapy. *Biomaterials* **2011**, *32*, 4976–4986. [CrossRef] [PubMed]

25.　Friedman, A.J.; Phan, J.; Schairer, D.O.; Champer, J.; Qin, M.; Pirouz, A.; Blecher-Paz, K.; Oren, A.; Liu, P.T.; Modlin, R.L.; et al. Antimicrobial and Anti-Inflamatory Activity of Chitosan-Alginate Nanoparticles: A Targeted Therapy for Cutaneous Pathogens. *J. Investig. Dermatol.* **2013**, *133*, 1231–1239. [CrossRef]

26.　Shahidi, S.; Wiener, J. Antibacterial Agents in Textile Industry. In *Antimicrobial Agents*; Bobbarala, V., Ed.; IntechOpen: London, UK, 2012.

27.　Kumar, M.N.; Muzzarelli, R.A.; Muzzarelli, C.; Sashiwa, H.; Domb, A.J. Chitosan Chemistry and Pharmaceutical Perspectives. *Chem. Rev.* **2004**, *104*, 6017–6084. [CrossRef]

28. Goyal, N.; Rastogi, D.; Jassal, M.; Agrawal, A.K. Chitosan as a Potential Stabilizing Agent for Titania Nanoparticle Dispersions for Preparation of Multifunctional Cotton Fabric. *Carbohydr. Polym.* **2016**, *10*, 167–175. [CrossRef]

29. Kadib, A.; Molvinger, K.; Guimon, C.; Quignard, F.; Brunel, D. Design of Stable Nanoporous Hybrid Chitosan/Titania as Cooperative Bifunctional Catalysts. *Chem. Mater.* **2008**, *20*, 2198–2204. [CrossRef]

30. Al-Sagheer, F.A.; Merchant, S. Visco-Elastic Properties of Chitosan–Titania Nano-Composites. *Carbohydr. Polym.* **2011**, *85*, 356–362. [CrossRef]

31. Xiao, W.; Xu, J.; Liu, X.; Huband, Q.; Huang, J. Antibacterial Hybrid Materials Fabricated Bynanocoating of Microfibril Bundles of Cellulosesubstance with Titania/Chitosan/Silver-Nanoparticle Composite Films. *J. Mater. Chem. B* **2013**, *1*, 3477. [CrossRef]

32. Kavitha, K.; Prabhu, M.; Rajendran, V.; Manivasankan, P.; Prabu, P.; Jayakumar, T. Optimization of Nano-Titania and Titania–Chitosan Nanocomposite to Enhance Biocompatibility. *Curr. Nanosci.* **2013**, *9*. [CrossRef]

33. Seco, A.M.; Gonçalves, M.C.; Almeida, R.M. Densification of Hybrid Silica–Titania Sol–Gel Films Studied by Ellipsometry and FTIR. *Mater. Sci. Eng. B* **2000**, *76*, 193–199. [CrossRef]

34. Matos, J.C.; Avelar, I.; Martins, B.; Gonçalves, M.C. Silica Vectors for Smart Textiles. *Carbohydr. Polym.* **2017**, *120*, 268–275. [CrossRef] [PubMed]

35. Gonçalves, M.C. Nanomaterials. In *Materials for Construction and Civil Engineering: Science, Processing, and Design*; Gonçalves, M.C., Margarido, F., Eds.; Springer: New York, NY, USA, 2015; pp. 629–677.

36. Murashkevich, A.N.; Lavitskaya, A.S.; Barannikova, T.I.; Zharskii, I.M. Infrared Absorption Pectra and Structure of TiO2-SiO2 Composites. *J. Appl. Spectrosc.* **2008**, *75*, 730. [CrossRef]

37. Mugundan, S.; Rajamannan, B.; Viruthagiri, G.; Shanmugam, N.; Gobi, R.; Praveen, P. Synthesis and Characterization of Undoped and Cobalt-Doped TiO2 Nanoparticles Via Sol–Gel Technique. *Appl. Nanosci.* **2015**, *5*, 449–456. [CrossRef]

38. Choudhury, B.; Choudhury, A. Luminescence Characteristics of Cobalt Doped TiO2 Nanoparticles. *J. Lumin.* **2012**, *132*, 178–184. [CrossRef]

39. Lacey, K.A.; Geoghegan, J.A.; McLoughlin, R.M. The Role of *Staphylococcus aureus* Virulence Factors in Skin Infection and Their Potential as Vaccine Antigens. *Pathogens* **2016**, *5*, 22. [CrossRef]

40. Taylor, T.A.; Unakal, C.G. Staphylococcus Aureus. In *StatPearls [Internet]*; StatPearls Publishing: Treasure Island, FL, USA, 2018.

41. Al Othman, Z.A.; Alam, M.M.; Naushad, M.; Khan, M.F. Inorganic Nanoparticles and Nanomaterials Based on Titanium (Ti): Applications in Medicine. *Mater. Sci. Forum* **2013**, *754*, 21–87. [CrossRef]

42. Arain, R.A.; Khatri, Z.; Memon, M.H.; Kim, I.S. Antibacterial Property and Characterization of Cotton Fabric Treated with Chitosan/AgCl-TiO$_2$ Colloid. *Carbohydr. Polym.* **2013**, *96*, 326–331. [CrossRef]

43. Gonçalves, M.C. Sol-Gel Silica Nanoparticles in Medicine: A Natural Choice. Design, Synthesis and Products. *Molecules* **2018**, *23*, 2021. [CrossRef]